

# Growth and Properties of Self Assembling Quantum Structures on GaAs Surfaces\*

P. M. Petroff

*Department of Materials, College of Engineering University of California, Santa Barbara, CA 93106-5050 USA*

Received July 12, 1993

This paper presents the methods that have been developed for directly growing quantum wires and quantum sized dots in III-V compound semiconductors. Both methods described in this paper rely on understanding and carefully controlling the growth kinetics during molecular beam epitaxy deposition. Ultra high density quantum wire arrays with dimensions below 10 nm have been obtained with the AlGaAs-GaAs and AlSb-GaSb systems and their one dimensional characteristics have been investigated by optical and magneto-optical techniques. Quantum sized dots have also been grown from InGaAs strained layers on GaAs surfaces. The transition of the two to three dimensional layer growth is detected by reflection high energy electron diffraction and is used to insure growth of a narrow size distribution of the InGaAs dots. The dot size and densities are adjustable. The structural and luminescence properties of these structures are presented.

## I. Introduction

Self assembling semiconductor structures offer an attractive approach for obtaining ultra high density arrays of quantum structures where carriers are two and three dimensionally confined. With the required confinement dimensions below few tenths of nanometers, the conventional lithography based techniques are indeed very difficult and time consuming to realize.

The direct growth of lateral superlattices (LSL) either by molecular beam epitaxy (MBE)<sup>[1,2]</sup> or metalorganic vapor deposition (MOCVD)<sup>[3]</sup> offers a new and rich range of opportunities for novel quantum structures and devices. These lateral superlattices are produced by depositing fractional monolayers of two semiconductors with different band gaps on an ordered vicinal surface and are used to produce quantum wire superlattices (QWS). With this approach, QWS showing a two dimensional carrier confinement have been realized for the GaAs-AlGaAs system<sup>[4]</sup>, the GaSb-AlGaSb system<sup>[5]</sup> and the InGaAs-InAlAs<sup>[6]</sup> pseudomorphic system.

Recent experiments on the LSL and QWS<sup>[4,5]</sup> have pointed out that the perfection of these structures relies heavily on a control of their growth kinetics and

of the deposition parameters, eg. flux uniformity, flux measurements. In this paper, we discuss the kinetic reactions that are presently limiting the perfection and properties of the as grown quantum wire superlattices. We present experimental evidence and Monte Carlo modeling of the deposition that provides good insight on the growth kinetics.

The direct growth of quantum dot structures has recently been pioneered by using selective growth on patterned GaAs substrates using MOCVD of AlGaAs and GaAs<sup>[7]</sup>. This technique relies on lithography and is limited by the dot density that can be obtained. The novel approach discussed in this paper makes use of a two to three dimensional growth transition to obtain a high density of quantum dots. This 2D to 3D growth transition is associated with the misfit strain of an InGaAs layer that is deposited on a GaAs substrate. The optical properties of these quantum dots are discussed.

## II. Lateral superlattices growth kinetics and optical properties

The direct growth of lateral superlattices such as the serpentine superlattices (SSL) or the tilted superlattice (TSL) has been used to produce quantum wire

\*Invited talk.

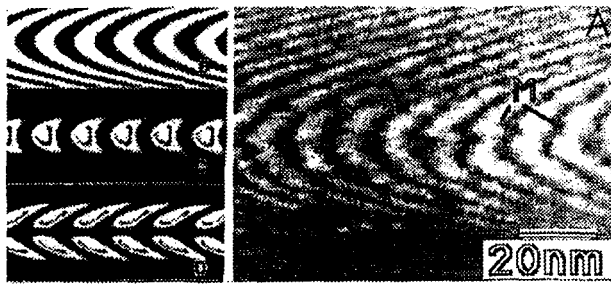


Figure 1: A) Cross section TEM micrograph of a single crescent SSL. Black represents areas that are GaAs rich while white regions correspond to the Al rich digital alloy barrier layers. Arrows in M indicate a meandering of the interface. B), C), and D) are respectively the computer simulated SSL structure B) and the computed density distributions of electrons confined to the ground state C) and first excited states D) (after reference<sup>[11]</sup>).

superlattices<sup>[1,4]</sup>. From the transmission electron microscopy (TEM) measurements and polarized photoluminescence measurements we have found that two sources of imperfections are present in these structures. The TEM micrograph in Fig. 1 identifies the roughness of the interfaces between the wells and barriers for an AlAs-GaAs serpentine superlattice as one of the problems. This interface roughness has been correlated through scanning tunneling microscopy (STM) studies<sup>[8,9]</sup> with the step edge roughness of the vicinal surface on which the LSL is deposited. Fig. 1 also indicates the nature of the second problem: the contrast between well and barrier regions is not as large as would be expected if the lateral compositional modulation was 100%. This poor lateral compositional modulation has also been detected by photoluminescence measurements<sup>[4,10]</sup>.

To understand the intermixing origin, we have explored the effects of elemental surface exchange reactions during growth. In fact, AlAs-GaAs short period superlattices e.g. monolayers or bilayers deposited by MBE on a (001) vicinal surface have been found to self organize into a lateral superlattices with a period corresponding to the step periodicity<sup>[12]</sup>. This self organization process into a LSL has also been found in the GaSb-AlSb and InGaAs-AlGaInAs short period superlattices<sup>[13]</sup>. Thus this self organization is a generic phenomenon which if understood could lead to improved LSL structures.

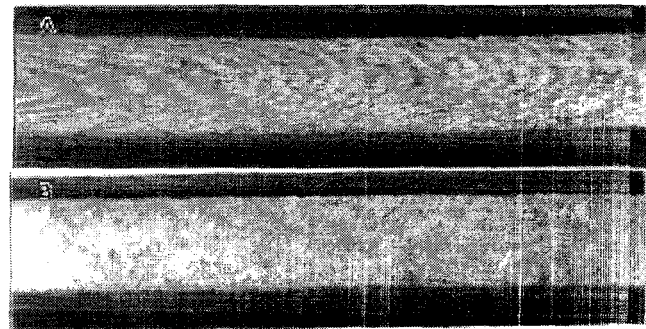


Figure 2: Cross section transmission electron micrograph of  $(\text{GaAs})_1 (\text{AlAs})_1$  short period superlattice grown in the ABE mode (A) and in the conventional MBE mode (B). In (A) a lateral superlattice with a period of -160 Å is clearly observed.

Our understanding of this self-organization is based on a series of experiments in which samples are grown by MBE on GaAs (001) substrates which are mis-oriented on  $1^\circ$  or  $2^\circ$  towards (111)A. The substrate temperature is  $600^\circ\text{C}$  and the As flux  $5 \times 10^{-6}$  Torr. The GaAs and AlAs growth rates are 0.21ML/s and 0.25ML/s respectively. The  $(\text{GaAs})_m (\text{AlAs})_n$  with  $m$  and  $n \leq 2$ , short period superlattices are grown either by conventional MBE or by alternate beam epitaxy (ABE)<sup>[14]</sup>. In the ABE deposition, the group V flux is shut off while the group III element flux is impinging on the surface. To compensate for measurement errors, in the growth flux, the serpentine superlattice flux ramping method<sup>[4]</sup> was adopted: the deposition parameter  $p = m + n$  is linearly varied with time from  $p = 1 - p_0$  to  $p = 1 + p_0$  with  $p_0 = 8\%$ . As shown in the TEM micrographs (Fig. 2a), the  $(\text{GaAs})_1 (\text{AlAs})_1$  superlattice deposited by MBE shows a random alloy with no chemical contrast modulation. However, the  $(\text{GaAs})_1 (\text{AlAs})_1$  superlattice in which the AlAs and GaAs are deposited in the ABE and MBE mode respectively shows a lateral superlattice (LSL) for the same deposition rate ramping (Fig.2b).

The chemical contrast modulation for this LSL is qualitatively similar to that of a conventional SSL<sup>[4]</sup>. This type of lateral modulation is observed whenever the deposition of the Al is taking place on an As depleted surface. The self organizing LSL has also been observed in GaSb-AlSb and InGaAs-AlInGaAs short

period superlattices for similar deposition conditions. We have proposed a surface exchange reaction to account for these observations. The Monte Carlo modeling of this process is based on the following assumptions:

a) the vicinal surface is composed of  $N$  steps with unit height monolayer. The deposition of Ga and Al is a random process and the atoms are not allowed to cross from one terrace to another. Periodic boundary conditions are used as previously described. The modeling is applied to the case of a constant coverage parameter with  $m = n = 1$ .

b) a reaction in which the impinging Al is exchanging place with a surface Ga atom is applied. The displaced Ga atom is then attached immediately to the terrace step rise: with no possibility of further exchange. An Al or a Ga atom impinging on an Al occupied surface site will not exchange. The atoms that have not exchanged are immediately attached to the step riser of the terrace.

Fig. 3a shows the deposition of alternate complete monolayers of AlAs (black dots) and GaAs (white arcs) in the case where no exchange reactions are present. The average chemical composition obtained for each atomic column is also shown. This ideal alternate monolayer superlattice does not exhibit any lateral composition modulation. The small fluctuations at the step edges are due to the random nature of the deposition.

Fig. 3b shows the simulation for the same growth sequence as that of Fig. 3a. with the exchange reaction process included. The average chemical composition obtained for each column is also plotted. A lateral compositional fluctuation that is similar in amplitude to that measured in the TEM micrograph is clearly observed (Fig. 2).

Exchange reactions between Al and Ga have been reported for AlAs deposited by MBE on GaAs {110} substrates<sup>[15]</sup> and for Al epitaxially deposited by MBE on GaAs {100} surfaces<sup>[16-18]</sup>. These thermodynamically driven exchange reactions which appear in a large number of heterostructure systems will therefore limit the lateral barrier heights in the QWS struc-

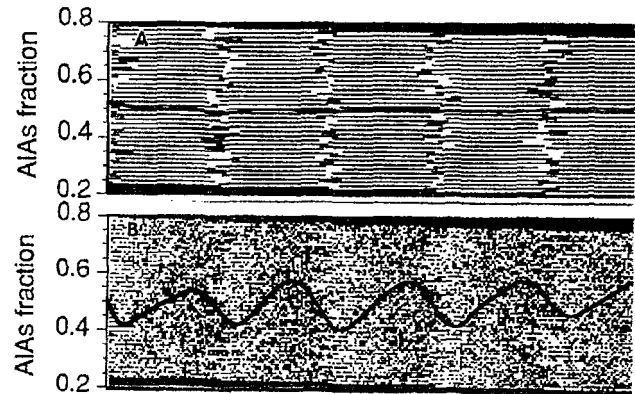


Figure 3: a) Monte Carlo simulation of a  $(\text{GaAs})_1(\text{AlAs})_1$  superlattice deposited on a vicinal surface with no exchange reaction included in the model. b) Monte Carlo simulation of the same superlattice. The superimposed line plots for these two simulations the AlAs fraction in each atomic column.

tures grown on vicinal surfaces. In fact, the polarized photoluminescence measurements carried out on the GaAs-Al<sub>0.3</sub>Ga<sub>0.7</sub>As QWS indicate a lateral barrier  $\Delta E_c = 70\text{meV}$  in the conduction band. The corresponding barrier and well material intermixing yield a difference in the Al content  $\Delta x = 0.1$  between the wire and barrier regions. Similar measurements on GaSb-AlSb QWS indicate a lateral barrier  $\Delta E_c = 350\text{meV}$  for the conduction electrons which translates into  $\Delta x = 0.3$  between the wire and barrier materials.

The weak lateral confinement for the conduction band electrons does not allow for the formation of a 1D subband in the GaAs-AlAs QWS. However, the  $\Delta x$  value is sufficient to produce a 2D confinement of the heavy holes. The low temperature magnetoluminescence properties of these quantum wire arrays have also been studied<sup>[19]</sup> in magnetic fields up to 10 Teslas. The diamagnetic shift from the SSL was found to be smaller than for a reference alloy quantum well with the same Al content, indicating an increase in the binding energy of the exciton due to the lateral confinement in the SSL structure. A diamagnetic shift anisotropy is observed when the magnetic field is applied in the three perpendicular directions of the wire. This is a direct observation of the one dimensional properties of the excitonic wave function. The PL line width increase with the applied magnetic field is dependent on

the direction of the applied field. These properties are consistent with the way the exciton volume is probing the potential variations in the SSL structure.

Obviously, improvements in the QWS structures produced by the direct growth method will depend on a better control of the growth kinetics and minimizing the surface exchange reactions.

### III. Growth and properties of self assembling quantum sized dots

The method uses the 2D to 3D transition during the initial growth of a highly strained  $\text{In}_{0.5}\text{Ga}_{0.5}\text{As}$  deposited by MBE on GaAs. This 2D to 3D transition corresponds to the formation of islands after an initial layer growth regime. This is the so called Stranski-Krastanov growth regime which has already been observed for In-GaAs on GaAs<sup>[20,21]</sup> and Ge on Si<sup>[22]</sup>. Within a narrow range of growth conditions, the islands may be grown free of misfit dislocations. The island nucleation comes as the first strain relief mechanism before the onset of misfit dislocation generation.

The samples are prepared by MBE and the  $\text{In}_{0.5}\text{Ga}_{0.5}\text{As}$  layer is grown at 530°C while the GaAs cladding layers were grown at 600°C and 450°C (for the top capping layer). The samples also include two  $\text{In}_{0.17}\text{Ga}_{0.73}\text{As}$  test quantum wells located 1000Å and 2000Å below the  $\text{In}_{0.5}\text{Ga}_{0.5}\text{As}$  layer. The  $\text{In}_{0.5}\text{Ga}_{0.5}\text{As}$  layer was deposited 0.5 monolayers at a time with a 0.5 second  $\text{As}_2$  pause repeated until the RHEED showed a transformation to a spotty pattern that indicate the 3D growth of islands on the surface. The transition from the 2 to 3D growth occurred after deposition of 3 monolayers.

The strain contrast observed in the TEM (Fig. 4) is characteristic of strain coherent centers with a radially symmetric strain field. The island size measured from the TEM micrographs is centered around 270Å with a remarkable size uniformity (gaussian distribution with a standard deviation of 28Å). The cross section TEM micrographs indicate the existence of the pseudomorphic  $\text{In}_{0.5}\text{Ga}_{0.5}\text{As}$  pseudomorphic layers and show that the island strain field is distributed in both cladding layers.

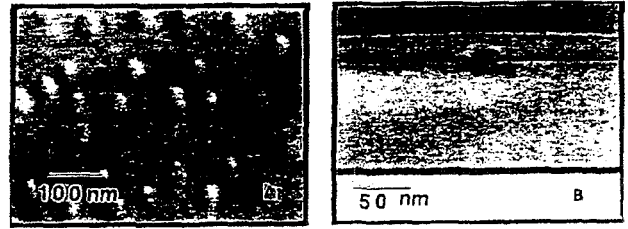


Figure 4: Transmission electron micrographs of coherently strained islands. a) Plan view and b) Cross section view of the samples.

The photoluminescence measurements carried out at 1.4°K with the 488nm line of an  $\text{Ar}^+$  ion laser indicate a strong luminescence from the  $\text{In}_{0.5}\text{Ga}_{0.5}\text{As}$  dot layer (Fig. 5) in addition to the two lines associated with the two test quantum wells. The sample with the pseudomorphic  $\text{In}_{0.5}\text{Ga}_{0.5}\text{As}$  layer only shows the luminescence from the two test quantum wells. The dot dimensions are small enough to produce quantum confinement. The presence of strain in the quantum dot structure produces a buried stressor structure which will induce a blue shift of the photoluminescence<sup>[23]</sup> in addition to the blue shift expected from the quantum confinement. Presently, the demonstration of OD confinement remains to be done in such structure, however the narrow size distribution and the excellent luminescence efficiency should enable this type of measurements to be performed in the near future.

Improvements in the growth kinetics understanding should enable an even narrower size distribution for the dot structures and permit a clear demonstration of the OD quantum size effects.

### IV. Conclusions

We have discussed two crystal growth methods that allow the direct processing of quantum wire superlattices and quantum sized dots structures in III-V compound semiconductors. The limitations and optical properties of these structures have been discussed.

### Acknowledgments

I wish to thank D. Leonard, C. Reaves, A. Lorke and M. Krishnamurthy for sharing some of their latest results with me. This research was sponsored by

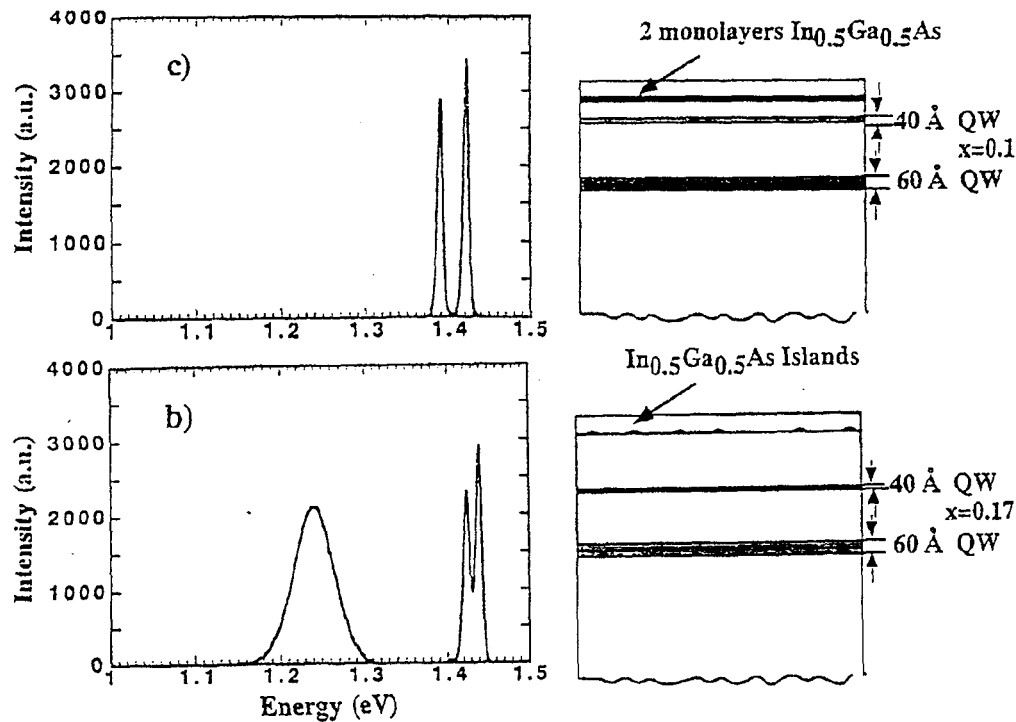


Figure 5: Photoluminescence spectra with their corresponding sample structure for two samples. The sample with the InGaAs dots shows a strong luminescence peak near 1.2eV.

QUEST an NSF-STC center (grant # 91-20007) and the AFOSR.

#### References

- J. Gaines, P. M. Petroff, H. Kroemer, R. J. Simes, R. S. Geels, and J. H. English J. Vac. Sci. Technol. B6, 1378 (1988).
- P. M. Petroff, A. C. Gossard and W. Wiegmann, Appl. Phys. Lett. (USA), 45, 620 (1984).
- T. Fukui, and H. Saito Appl. Phys. Lett. 50, 824 (1987).
- M. S. Miller, H. Weman, C. E. Pryor, M. Krishnamurthy, P. M. Petroff, H. Kroemer, and J. L. Merz, Phys. Rev Lett. 68, 3464 (1992).
- S. Chalmers, H. Weman, J. C. Yi, H. Kroemer, J. L. Merz, and N. Dagli. Appl. Phys. Lett. 60, 1676 (1992).
- D. Leonard (private communication).
- T. Fukui, S. Ando, and H. Saito, Science and Technology of Mesoscopic Structures, edited by S. Namba, C. Hamaguchi, and T. Ando, (Springer Verlag, Tokyo, 1992) p. 353.
- K. Pond, R. Maboudian, V. Bressler-Hill, D. Leonard, X. S. Wang, K. Self, W. H. Weinberg, and P. M. Petroff. J. Vac. Sci. Technol. B (to be published 1993).
- A. Poudoulec, B. Guenas, C. d'Anteroches, P. Auvray, and A. Regeny. Appl. Phys. Lett. 60, 2406 (1992).
- S. A. Chalmers, A. C. Gossard, P. M. Petroff and H. Kroemer J. Vac. Sci. Technol. B8, 431 (1990); S. A. Chalmers, H. Kroemer and A. C. Gossard Appl Phys. Lett. 57, 1751 (1990).
- J. C. Yi, N. Dagli and L. A. Coldren Appl. Phys. Lett. 59, 3015 (1991).
- M. Krishnamurthy, A. Lorke and P. M. Petroff, J. Vac. Sci. Technol. B (1993).
- M. Krishnamurthy, A. Lorke and P. M. Petroff (to be published).
- Y. Horikoshi, Y. Yamaguchi, F. Briones, and M. Kawashima. J. Cryst. Growth 105, 326 (1990).
- R. Ludeke and G. Landgren. J. Vac. Sci. Technol. 19, 667 (1981).
- R. Ludeke, J. Vac. Sci. Technol. B 2, 400 (1984).
- J. M. Moison, F. Houzay, F. Barthe, J. M. Gerard, B. Jusserand, J. Massies and F. S. Turco Sandroff.

- J. Cryst. Growth **111**, 141 (1991).
18. B. Jusserand, and F. Mollot, Appl. Phys. Lett. **61**, 423 (1992).
  19. H. Weman, E. Jones, C. McIntyre, M. Miller, P. Petroff, and J. Merz. J. of Superlattices and Microstructures (1992).
  20. C. W. Snyder, B. G. Orr, D. Kessler and L. M. Sander. Phys. Rev. Lett. **66**, 3032 (1991).
  21. D. Leonard, M. Krishnamurthy, C. Reaves, S. Denbaars and P. M. Petroff. (submitted for publication).
  22. M. Krishnamurthy, J. S. Drucker, and J. A. Venables J. Appl. Phys. **69**, 6461 (1991).
  23. Z. Xu and P. M. Petroff, J. Appl. Phys. **69**, 6564 (1991).